

Pressure-induced staging transition in TiS_2 intercalation compounds

Otto Zhou and John E. Fischer

*Department of Materials Science and Engineering and Laboratory for Research on the Structure of Matter,
University of Pennsylvania, Philadelphia, Pennsylvania 19104*

Keng S. Liang

Corporate Research Science Laboratory, Exxon Research and Engineering Company, Annandale, New Jersey 08801

(Received 9 May 1991)

Single-crystal diamond-anvil x-ray diffraction at 300 K reveals a reversible stage-1-to-stage-2 transition in $\text{Ag}_{0.35}\text{TiS}_2$, with an onset pressure < 1 kbar and coexisting stages up to 25 kbar. In contrast, no stages higher than 1 are observed in $\text{Li}_{0.5}\text{TiS}_2$ up to 55 kbar. We argue that the different behavior of Li and Ag intercalates cannot be understood in terms of a continuum elastic model but depends instead on the different interatomic distances and atomic radii.

Layer intercalates exhibit a rich variety of structures as functions of the thermodynamic variables T , P , and chemical potential μ .¹⁻⁴ A particular example is the effect of hydrostatic pressure on the stage index (i.e., the periodic sequence of filled and empty galleries) in graphite intercalation compounds (GIC's). At constant T and μ , pressure-induced staging transitions are found to be mainly driven by the PV term in the free energy; it is more favorable to densely fill a fraction of the van der Waals galleries than to sparsely occupy all of them because a filled gallery is thicker than an empty one.⁵

Pressure-induced staging transitions have been extensively studied in graphite intercalation compounds.^{5,6} In one case, the same transition was observed at low T and high P , and the experimental (P, T) slope agrees with a Clausius-Clapeyron estimate, which neglects changes in internal energy, e.g., associated with commensurate in-plane lock in.^{7,8} This implies that the model developed by Safran and Hamann⁹ and Safran¹⁰ to explain the existence of different stages versus T , and μ can be at least qualitatively applied to P -induced transitions as well. In this model, the T (or P) scale of the phase boundaries is set by U_0 , an effective two-body in-plane attractive interaction, which is mediated by local elastic distortions of the host layers around an intercalate. U_0 scales approximately as R/L^2 , where R is the intercalate radius and L is the in-plane "healing length" of the distortion, which depends only on the host elastic properties.¹¹⁻¹⁴ This framework provides a qualitative explanation for the existence of stage transitions versus μ in Li_xC_6 at 300 K, 1 atm, and their absence in Li_xTiS_2 . The stiffer host layers in the latter compound result in a larger L and thus smaller U_0 , so 300 K lies above all the phase boundaries. Low- T powder neutron diffraction showed that dilute stage-1 $\text{Li}_{0.5}\text{TiS}_2$ is at least metastable down to 170 K, indicating either that U_0 for Li in TiS_2 is less than 570 K or that restaging is kinetically hindered.¹⁵ Similarly, low- T x-ray studies of Ag_xTiS_2 show no evidence for restaging down to 10 K.¹⁶ On the other hand, a high-temperature transition from stage-2 to stage-1 (qualitatively consistent

with the Safran model) has been reported for Ag_xTiS_2 .^{17,18}

In fact, staging transitions are generally ubiquitous in GIC's but are quite rare in transition-metal dichalcogenide intercalation compounds (TMDIC). In this paper we report preliminary results of a study of pressure-induced staging transitions in Li- and Ag-intercalated TiS_2 , a prototype transition-metal dichalcogenide (TMD). TiS_2 consists of triple-layer S-Ti-S sandwiches with strong internal covalent bonds, weakly held together by van der Waals interactions.¹⁹ Li and Ag intercalates both occupy octahedral sites in the van der Waals galleries.^{19,20} As noted above, Li_xTiS_2 is limited to stage-1 at 300 K, 1 atm, for $0 < x < 1$, while higher stages have been reported for dilute Ag_xTiS_2 .^{21,22} In this work, we find that stage-1 $\text{Li}_{0.5}\text{TiS}_2$ is stable up to 55 kbar at 300 K, while $\text{Ag}_{0.35}\text{TiS}_2$ begins transforming to stage-2 at less than 2 kbar. This large difference in threshold pressures cannot be readily explained with the continuum elasticity approach, which works qualitatively for GIC's.

Single-crystal $\text{Ag}_{0.35}\text{TiS}_2$ was prepared by reacting Ag and TiS_2 powders in a vacuum sealed quartz ampoule for three days at 1000°C, then cooling slowly to room temperature. Chemical composition was determined by energy-dispersive x-ray analysis in a scanning microscope. X-ray diffraction showed no detectable stages other than stage 1; the 300 K, 1 atm., lattice parameters were $c=6.390$ and $a=3.418$ Å. $\text{Li}_{0.5}\text{TiS}_2$ powder was prepared by reacting proportional amounts of TiS_2 and *n*-butyllithium in hexane at 300 K, followed by homogenization in lithium perchlorate and acetonitrile. The c parameter expanded from 5.69 to 6.116 Å, from which $x=0.5$ was determined by comparison with published results.¹⁹

We used a standard Merrill-Bassett diamond-anvil cell^{23,24} with CaF_2 powder as a pressure standard and pentane-isopentane hydrostatic pressure medium for Li_xTiS_2 and methanol-ethanol for Ag_xTiS_2 . $\text{Li}_{0.5}\text{TiS}_2$ powder was studied using a standard circular gasket hole.

Two different arrangements were necessary for the single-crystal Ag_xTiS_2 experiment in order to record ($HK0$) and ($00L$) reflection families. The crystals grow as thin flakes with c parallel to the thin dimension. For ($HK0$)'s, a crystal was placed flat on the culet in a circular gasket hole. For ($00L$)'s we spark cut a rectangular slot 0.13×0.43 mm through a 0.2-mm-thick T301 stainless steel gasket, then attached a crystal ($0.2 \times 0.1 \times 0.01$ mm) inside the slot with the c axis perpendicular to the slot and parallel to the culet. This ensures that the crystal remains close to the initial orientation as the pressure is increased. The drawback is that the slot closes nonuniformly at about 30 kbar, and an increasing fraction of the ($00L$) intensity is occluded by the gasket as P increases. X-ray experiments were performed on the Exxon X10A and X10B beamlines at the National Synchrotron Light Source, Brookhaven National Laboratory, NY.

As noted above, the $\text{Ag}_{0.35}\text{TiS}_2$ was pure stage 1 before loading in the diamond-anvil cell. The minimal pressure necessary to seal the gasket (< 1 kbar) was sufficient to initiate the onset of stage 2, as revealed by a new reflection at 1.031 \AA^{-1} [(002), $c = 12.189 \text{ \AA}$]. Above 2 kbar, additional new peaks with Q values corresponding to (001), (003), and (006) reflections of the stage-2 phase are also observed. Figure 1 shows data in the Q range covering the stage-1 (001) and stage-2 (002) at five pressures, along with fits to two Gaussians plus a quadratic background. The maximum count rate decreased continuously with increasing P due to the closing up of the slot, so in Fig. 1 we normalized each profile to a constant total integrated Bragg intensity. It is clear that the stage-2 (002) grows with increasing P at the expense of the stage-1 (001), with no stage 1 remaining at 22.8 kbar. The stage-1 (001) shows no P -induced broadening; the out-of-plane coher-

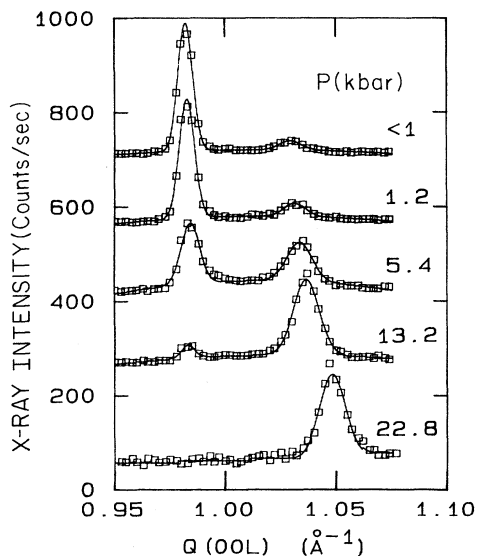


FIG. 1. Stage-1 (001) and stage-2 (002) peaks of $\text{Ag}_{0.35}\text{TiS}_2$ at five pressures, along with fits to two Gaussians plus a quadratic background. Each profile is normalized to a constant total integrated Bragg intensity.

ence length is about 800 \AA , estimated by the Scherrer formula. Conversely, the stage-2 (002) first emerges with a width about 1.5 times greater than the stage-1 value, then broadens slightly more with increasing P . Diffuse scattering builds up between the Bragg peaks at intermediate P , as seen from the P dependence of the background parameters (in particular at 5.4 kbar), and then disappears at higher P as stage 2 becomes a pure phase.

The evolution of stage 2 with increasing pressure was found to be continuous. The two phases coexist over the range $1 < P < 23$ kbar, as shown in Fig. 2. Here we approximate the relative amount of each phase by the integrated intensity from the Gaussian fits to Fig. 1, which in effect neglects differences in structure factors $S(00L)$ and the contribution of a possibly P -dependent in-plane Ag concentration to $S(00L)$. Repeat scans after increasing pressure show that the system reaches equilibrium (or quasi-equilibrium) in less than 30 min. The transition is reversible; releasing the pressure restores an essentially pure stage-1 profile.

In order to look for evidence of in-plane Ag ordering, we also recorded ($HK0$) profiles for the same range of pressures, using a different $\text{Ag}_{0.35}\text{TiS}_2$ crystal from the same batch. Data and fits in the Q region of the $\text{Ag}_{0.35}\text{TiS}_2$ (100) are shown in Fig. 3. In contrast to the ($00L$) experiment, the ($HK0$) scattering volume is essentially independent of pressure, thus absolute intensity variations with P convey useful information. At < 1 kbar the (100) is well-represented by a single resolution-limited Gaussian (coherence length $> 1600 \text{ \AA}$), with $a = 2.961(7) \text{ \AA}$ in good agreement with the literature value for stage 1. Increasing P to 3.4 kbar shows a small compressibility effect and a 30% drop in integrated intensity. At 19.1 kbar the (100) has two broad components (coherence length about 800 \AA) whose d values differ by 0.013 \AA , close to the difference between stage-1 and stage-2 in-plane lattice constants at 1 atm.²¹ Less than 1/3 of the initial total integrated intensity remains at this P . Only a very weak low- Q component persists at 23.7 kbar, while

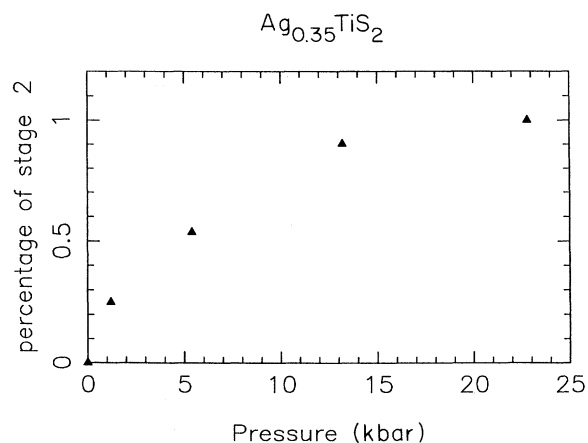


FIG. 2. Evolution of stage-2 $\text{Ag}_{0.35}\text{TiS}_2$ with increasing pressure, estimated by the integrated intensity from the Gaussian fits to Fig. 1.

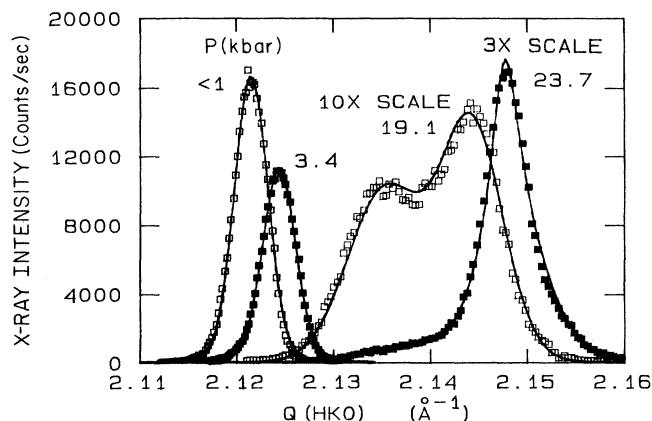


FIG. 3. Data and fits in the Q region of the $\text{Ag}_{0.35}\text{TiS}_2(100)$ reflection for four pressures.

the high- Q component has sharpened overall but now shows power-law tails (represented in the fit by a mixed Lorentzian-Gaussian line shape). The integrated intensity has increased slightly from its value at the previous pressure.

It is apparent from Fig. 3 that the P dependence of the stage-1 and stage-2 (100) relative intensities differs quantitatively from the (00L) results. For example, at 19 kbar the stage-2 (100) fractional intensity is about 0.5, while from Fig. 2 the corresponding (00L)-derived value is about 0.9. Part of this discrepancy may be related to the P -dependent total integrated intensity noted above. The (100) radial intensity is sensitive to stacking faults in the $1T$ polytype structure of the host material, so one possibility is that the staging transition involves, or is mediated by, faults that “heal” as a pure high- P phase is achieved. A second possibility is that the in-plane Ag concentration varies differently with P in the two phases. We found no evidence for P -induced in-plane Ag ordering, but the possibility remains that a variable “coverage” of Ag on lattice gas sites could lead to a P -dependent $S(100)$. A similar effect has been observed for disordered Li in graphite.²⁵ A third possibility is that the two samples take different paths through the two-phase coexistence region.

In contrast to $\text{Ag}_{0.5}\text{TiS}_2$, a powder sample of $\text{Li}_{0.5}\text{TiS}_2$ showed no evidence of staging or polytype transitions up to 55 kbar. The peak positions were consistent at all pressures with the $1T$ stage-1 structure. We cannot rule out the possibility of P -induced modifications involving only the relative Bragg intensities, because the flaky powder takes on a strongly preferred orientation, which exaggerates the $(HK0)$'s relative to $(00L)$'s at high P .

In Table I we collect compressibility values $K_c = \Delta c / c$ and $K_a = \Delta a / a$ per kbar for the compounds discussed above, as well as our results for pristine TiS_2 powder. For both TiS_2 and $\text{Li}_{0.5}\text{TiS}_2$, K_c is roughly four times greater than K_a as expected for layer structures. Comparison of values for these two materials shows that occupying half the octahedral sites with Li has only a minor stiffening effect in both directions. Stage-2 $\text{Ag}_{0.15}\text{TiS}_2$ is

TABLE I. Compressibility (10^{-3} kbar) of $M_x\text{TiS}_2$.

	TiS_2	$\text{Li}_{0.5}\text{TiS}_2$ stage 1	$\text{Ag}_{0.15}\text{TiS}_2$ stage 2	$\text{Ag}_{0.35}\text{TiS}_2$ stage 1	$\text{Ag}_{0.35}\text{TiS}_2$ stage 2
K_c	1.71 (1.83 ^a)	1.53	1.96	0.23	0.88
K_a	0.56	0.44		0.39	0.37

^aReference 29.

actually softer in the c direction than the undoped material, indicating that the decreased van der Waals interaction due to the larger c parameter overrides the ionic component of interlayer bonding associated with electron transfer from Ag to TiS_2 layers. In all three materials K_c is essentially independent of P . Since a staging transition occurs in $\text{Ag}_{0.35}\text{TiS}_2$, the K_c values in principle include offsetting contributions from the true compressibility and from P -dependent in-plane density, which affects the thickness of an occupied gallery. Thus the value 0.23×10^{-3} for the stage-1 component at low P probably reflects the tradeoff between emptying the galleries to “feed” the emerging stage-2 (an effective $K_c < 0$), and a true compressibility not much different from the others. Similarly, the 0.88×10^{-3} value for the stage-2 component, derived from the 19.1 and 23.7 kbar profiles in Fig. 3, is probably close to saturating at a value characteristic of the true stage-2 compressibility, since the filling of the stage-2 galleries is nearing completion. It would be interesting to extend these measurements to higher P in order to measure the true compressibility of stage-2 “ $\text{Ag}_{0.70}[\text{TiS}_2]_2$ ”; the presence of the (presumably soft) empty gallery can be corrected for by using the K_c of TiS_2 . Similarly, measurements on stage-1 $\text{Ag}_{0.35}\text{TiS}_2$ with higher P resolution and at low P may give the true compressibility. The combination could then be used to determine the coverage-dependent compressibility of octahedral Ag layers.

The differences in c -axis compressibility K_c and staging transition threshold pressure between $\text{Li}_{0.5}\text{TiS}_2$ and $\text{Ag}_{0.35}\text{TiS}_2$ are discussed here in terms of S- M ($M = \text{Li, Ag}$) bonding distances and Li^+ and Ag^+ ionic radii. To first order, the covalently bonded MX_2 sandwiches are treated as rigid incompressible blocks, which leaves the change of interblock distance as the only contribution to K_c . We take $a/2 = 1.71 \text{ \AA}$ as the effective sulfur radius.²⁶ It follows that the radius of the vacant octahedral site in the van der Waals gap of pristine TiS_2 is 0.72 \AA . Shannon gives 1.01 \AA for the radius of Ag^+ .²⁷ Silver intercalation to $x = 0.35$ expands c from 5.69 to 6.39 \AA , and a lattice refinement²² gives a Ag-S distance of 2.66 \AA with Ag midway between two adjacent blocks. This is slightly smaller than 2.72 \AA , the sum of Ag and S radii in this crude estimate, but it suggests that the S-Ag-S octahedron is already closely packed at 1 atm. A similar estimate shows that the Li-S interatomic distance is 2.57 \AA in $\text{Li}_{0.5}\text{TiS}_2$ at 1 atm, about 0.2 \AA larger than the sum of Li^+ and S radii (2.38 \AA). This explains the similarity of K_c values for pristine TiS_2 and $\text{Li}_{0.5}\text{TiS}_2$; for small c -axis compressions, adjacent host blocks do not “feel” the Li as they are compressed.

In a hard sphere picture, the difference in threshold pressures for restaging in Ag- and Li-intercalated TiS_2 is a direct consequence of the close packing of Ag and S in the former and the availability of free space between Li and S in the latter. According to Le Chatelier's principle, a system under pressure will reduce its volume to minimize the free energy $F=U-TS+PV$. In intercalation compounds, this can be accomplished initially, at low P , by compressing the interblock spacing. The P range over which this dominates depends upon the initial free space at 1 atm and the compressibility of the system. Then, after adjacent atoms come into contact with increasing P , further c axis compression may be achieved by a transformation to a higher stage, since the specific volume per intercalate is reduced. This defines the threshold pressure, which therefore depends on U_0 , electrostatic interactions between intercalates, and the temperature.

A low transition pressure is expected in host lattices with larger U_0 because high P and low T are inversely related, as discussed above. Intercalate size and host layer rigidity affect the transition pressure through U_0 , which scales as R/L^2 in a simple continuum model.¹² Electrostatic interactions must also play a role in the T - and P -dependent phase equilibria, but these have not been explicitly incorporated in the current models. In the present case the threshold pressure is also expected to be temperature-dependent because, in a stage-1-to-stage-2 transition, the configurational entropy will be reduced due to the increased occupancy of previously vacant octahedral sites. At elevated temperature, the TS term will dominate the free energy, leading to an increase in threshold pressure.

Our estimate, showing that the S-Ag-S octahedron is closely packed at 1 atm. is consistent with the small K_c value of stage-1 $\text{Ag}_{0.35}\text{TiS}_2$, which is even smaller than K_a . We estimate that $\text{Li}_{0.5}\text{TiS}_2$ will similarly achieve close packing at 65 kbar by extrapolating the K_c data. The present results were limited to 55 kbar; further work is underway to study the behavior of Li_xTiS_2 in the 100 kbar range with a different cell. The absence of higher stages in stage-2 $\text{Ag}_{0.15}\text{TiS}_2$ ($a=3.406 \text{ \AA}$, $c=12.153 \text{ \AA}$ at 300 K, 1 atm) up to 29 kbar, studied in a similar experiment, can also be understood by the same argument. In

stage 2, alternating van der Waals galleries are occupied and empty, and the empty gallery has very large K_c (close to TiS_2) and thus acts as a "buffer" in volume reduction. Restaging will begin only after the empty gallery is compressed to the point that sulfur-sulfur repulsion is strong enough to prevent further contraction between adjacent TiS_2 blocks.

The large difference in threshold pressures between Li- and Ag-intercalated TiS_2 is inconsistent with an elastic continuum model. The ratio $U_0(\text{Ag})/U_0(\text{Li})$ for Ag and Li in TiS_2 is predicted to be 1.5 based on the scaling described above. This is much smaller than 28, the experimental lower bound from the present results, indicating that mean field phase diagrams and continuum results cannot simply be extended from GIC's to TMDIC's without some modification. One essential difference between these two material families is the host layer stiffness. In GIC's, electrostatic interactions are negligible in comparison with elastic dipole interactions, partly due to the "softness" of graphite host layers. TMD's are much stiffer; electrostatic interactions play a role in defining the local atomic structure, and may therefore contribute to the energetics of staging transitions in TMDIC's.²⁸

The observation of pressure-induced restaging in $M_x\text{TiS}_2$ implies the existence of a microscopic mechanism with reasonable kinetics at 300 K. This is provided in graphite intercalates by Daumas-Hérolld domains,³⁰ which require elastic deformations of host layers.³¹ We have shown for TiS_2 that the energetics of restaging, in particular the large difference in threshold pressure between Ag and Li, cannot be accounted for by elastic considerations. By implication, there must exist a different microscopic mechanism by which restaging can occur in TMDIC's. Elastic property measurements of TiS_2 would be helpful to make quantitative comparisons of restaging in the two systems.

We are grateful to H. E. King, Jr., A. Jayaraman, and A. Ruoff for advice and assistance in high-pressure techniques, and to D. Murphy for advice on Li_xTiS_2 sample preparation. This work was supported by Department of Energy (DOE) Grant No. DEFG02-87ER45254.

¹J. E. Fischer and T. E. Thompson, *Phys. Today* **31**, 36 (1978).

²Proceedings of International Symposium on Graphite Intercalation Compounds, Tsukuba, Japan, 1985 [*Synth. Met.* **12**, (1985)].

³*Intercalation in Layered Materials*, Vol. 148 of *NATO Advanced Studies Institute, Series B: Physics*, edited by M. S. Dresselhaus (Plenum, New York, 1986).

⁴Proceedings of the International Symposium on Graphite Intercalation Compounds, Jerusalem, 1987 [*Synth. Met.* **23**, (1987)].

⁵R. Clarke, N. Wada, and S. A. Solin, *Phys. Rev. Lett.* **44**, 1616 (1980).

⁶H. J. Kim, J. E. Fischer, D. B. McWhan, and J. D. Axe, *Phys. Rev. B* **33**, 1329 (1986).

⁷J. E. Fischer, C. D. Fuerst, and K. C. Woo, *Synth. Met.* **7**, 1 (1983).

⁸D. P. DiVincenzo, C. D. Fuerst, and J. E. Fischer, *Phys. Rev. B* **29**, 1115 (1984).

⁹S. A. Safran and D. R. Hamann, *Phys. Rev. Lett.* **42**, 1021 (1979).

¹⁰S. A. Safran, *Phys. Rev. Lett.* **44**, 940 (1980).

¹¹J. R. Dahn, D. C. Dahn, and R. R. Haering, *Solid State Commun.* **42**, 179 (1982).

¹²J. E. Fischer and H. J. Kim, *Phys. Rev. B* **35**, 3295 (1987).

¹³S. Lee, H. Miyazaki, S. D. Mahanti, and S. A. Solin, *Phys. Rev. Lett.* **62**, 3066 (1989).

¹⁴M. F. Thorpe, W. Jin, and S. D. Mahanti, *Phys. Rev. B* **40**, 10294 (1989).

- ¹⁵T. P. Feist and J. E. Fischer (unpublished).
- ¹⁶Y. Kuroiwa, K. Ohshima, and Y. Watanabe, *Phys. Rev. B* **42**, 11 591 (1990).
- ¹⁷K. K. Bardhan, G. Kirczenow, G. Jackle, and J. C. Irwin, *Phys. Rev. B* **33**, 6 (1986).
- ¹⁸G. L. Burr, V. G. Young, Jr., M. J. McKelvy, W. S. Glaunsinger, and R. B. Von Dreele, *J. Solid State Chem.* **84**, 355 (1990).
- ¹⁹M. S. Whittingham, *Prog. Solid State Chem.* **12**, 41 (1978).
- ²⁰R. H. Friend and A. D. Yoffe, *Adv. Phys.* **36**, 1 (1987).
- ²¹G. A. Scholz and R. F. Frindt, *Mater. Res. Bull.* **15**, 1703 (1980).
- ²²A. G. Gerards, H. Roeder, R. J. Haanger, B. A. Boukamp, and G. A. Wiegers, *Synth. Met.* **10**, 51 (1984).
- ²³L. Finger and R. Hazen, *Comparative Chemistry* (Wiley, New York, 1982).
- ²⁴A. Jayaraman, *Rev. Mod. Phys.* **55**, 1 (1983).
- ²⁵H. J. Kim, A. Magerl, J. L. Soubeyroux, and J. E. Fischer, *Phys. Rev. B* **39**, 4670 (1989).
- ²⁶F. R. Gamble, *J. Solid State Chem.* **9**, 358 (1974).
- ²⁷R. D. Shannon, *Structure and Bonding in Crystals*, edited by M. O'Keeffe and A. Navrotsky (Academic, New York, 1981), Vol. II.
- ²⁸M. Mori, K. Ohshima, S. C. Moss, R. F. Frindt, M. Plishke, and J. C. Irwin, *Solid State Commun.* **43**, 781 (1982).
- ²⁹M. Sharli and F. Levy, *Phys. Rev. B* **33**, 6 (1986).
- ³⁰N. Daumas and A. Hérold, *C. R. Acad. Sci. Ser. C* **268**, 373 (1963).
- ³¹S. Ulloa and G. Kirczenow, *Phys. Rev. Lett.* **52**, 218 (1985).